EurJIC
European Journal of Inorganic Chemistry

Research Article
doi.org/10.1002/ejic.202200174

Chemistry Europe
European Chemical Societies Publishing

www.eurjic.org

Ortho-F,F-DPEphos: Synthesis and Coordination Chemistry in Rhodium and Gold Complexes, and Comparison with DPEphos

James J. Race,*[a, b] Matthew J. Webb,[a] Timothy Morgan Boyd,[a, b] and Andrew S. Weller*[a]

The synthesis of a new *ortho*-fluorine substituted diphosphine ligand based upon the DPEphos ligand is reported: *o*-F,F-DPEphos (DPEphos = bis(2-diphenylphosphinophenyl)ether). The corresponding bimetallic gold complex Au_2Cl_2(*o*-F,F-DPEphos) and Schrock-Osborn type Rh(I) complex [Rh(*o*-F,F-DPEphos)(NBD)][BAr^F_4] have been synthesized (Ar^F = 3,5-$(CF_3)_2$-C_6H_3). The solid-state and solution phase NMR data are examined in comparison with the *o*-H,H-DPEphos equivalents, and demonstrate the influence of *ortho*-fluorine substitution through the control of aurophilic and Rh···X interactions (X=H or F). Characterization of the organometallic products upon hydrogenation of the Schrock-Osborn complexes in 1,2-$F_2C_6H_4$ revealed a Rh dimeric complex [Rh(H)(*fac*-κ³-P,O,P-μ-CH-DPEphos)]$_2$[BAr^F_4]$_2$ with a bridging C–H agostic interaction for the parent DPEphos. The substituted variant formed a Rh(III) monomer [Rh(*mer*-κ³-P,O,P-*o*-F,F-DPEphos)H_2][BAr^F_4], highlighting the structural consequences of *ortho*-fluorine substitution.

Introduction

The manipulation of the steric and electronic properties of phosphine ligands is a well-known method for tuning reactivity and selectivity in transition-metal mediated catalysis.[1,2] *Ortho*-substitution at phosphorus aryl-substituents is one method to do this, and there are a number of examples of how *ortho*-functionalization can affect the coordination geometry,[3] reactivity[4–6] and selectivity of homogeneous catalysts.[7–10] *Ortho*-fluorine substitution, however, is much rarer.[11,12] *Ortho*-aryl fluorine substitution has been used to increase the rate of biphenyl reduction in Pt(Ph)$_2$(*o*-F-diphosphine) complexes,[13] and shown to increase catalyst productivity in Cr-catalyzed ethylene oligomerisation.[14,15] DPEphos (DPEphos = bis(2-diphenylphosphinophenyl)ether, named *o*-H,H-DPEphos here for clarity, Figure 1A), is an example of a POP-type diphosphine ligand that can be readily adapted by changing the phosphorus substituents.[16,17] Initially synthesized for use as a κ²-P,P wide bite-angle diphosphine ligand for selective hydroformylation catalysis,[18] *o*-H,H-DPEphos has since been shown to coordinate to a transition metal atom in a variety of geometries, including:

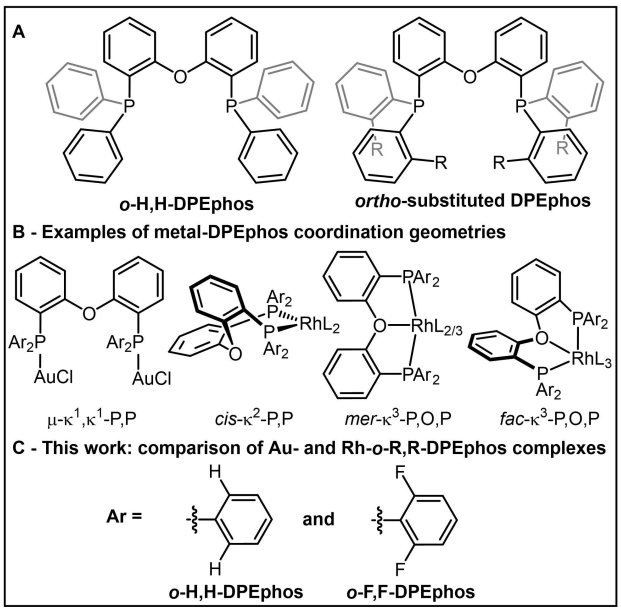

Figure 1. A) *o*-H,H-DPEphos and *ortho*-substituted DPEphos. **B**) Some examples of the coordination modes of DPEphos in metal-DPEphos complexes. **C**) The work reported in this article – a comparison of the rhodium and gold coordination chemistry of *o*-H,H-DPEphos and *o*-F,F-DPEphos.

[a] J. J. Race, M. J. Webb, T. Morgan Boyd, Prof. A. S. Weller
Department of Chemistry
University of York
Heslington, YO10 5DD, UK
E-mail: jjr534@york.ac.uk
andrew.weller@york.ac.uk
[b] J. J. Race, T. Morgan Boyd
Chemistry Research Laboratories
University of Oxford
Oxford, OX1 3TA, UK

Supporting information for this article is available on the WWW under https://doi.org/10.1002/ejic.202200174

μ²,κ¹,κ¹-P,P, κ²-P,P and κ³-P,O,P (Figure 1B).[19] This coordination flexibility, facilitated by the hemilabile[19] nature of the oxygen, has been demonstrated in a range of homogeneous catalytic processes. For example the Pd(*o*-H,H-DPEphos)-catalyzed Suzuki cross-coupling to form sterically hindered biaryls[20] and aryl-phosphonates,[21] or amination of allylic alcohols using a Pt(*o*-H,H-DPEphos)Cl_2 precatalyst.[22] The cationic [Rh(*o*-H,H-DPEphos)]$^+$ system has been employed to catalyze alkene and alkyne intermolecular hydroacylation[23–25] and amine-borane

Research Article
doi.org/10.1002/ejic.202200174

dehydropolymerization.[26,27] Transitioning between the possible coordination modes has been shown to be important for catalytic activity in some cases.[23,25,28] Examples of aryl modification in DPEphos are rare, and catalytic applications, thus far, are limited.[16,29–33] Most recently, rhodium Schrock-Osborn type[34,35] precatalysts containing *ortho*-aryl-substituted DPEphos ligands have been reported, in which steric bulk was varied [Rh(R-DPEphos)(NBD)][BAr^F_4] (R = H, Me, OMe, ^{i}Pr; NBD = norbornadiene and Ar^F = 3,5-$(CF_3)_2$-C_6H_3).[17] Changes in the steric properties of the *ortho*-substituent influenced the coordination geometry and further reactivity of the precatalyst upon hydrogenation of the norbornadiene fragment. For example, the identification of Rh···H–C anagostic[36] interactions in the NBD complexes and ligand C–H activation in the (R = ^{i}Pr) when activated using dihydrogen. In light of these studies, and wanting to explore the wider scope of *ortho*-aryl substitution in DPEphos ligands, we now report the synthesis of *ortho*-F,F-DPEphos (Figure 1C), in which the *ortho*-phenyl hydrogen atoms in parent DPEphos have been replaced with fluorine, and preliminary coordination chemistry studies with Au and Rh-centers. The influence of this *ortho*-fluorine substitution switches off solid-state aurophilic interactions in the bimetallic Au(I) complex Au_2Cl_2(*o*-F,F-DPEphos) compared to the *o*-H,H-DPEphos equivalent;[37] while in the Schrock-Osborn type precatalyst,[34,35] [Rh(*o*-F,F-DPEphos)(NBD)][BAr^F_4], *ortho*-fluorine substitution stops the formation of hydride-bridged dimers upon hydrogenation, for which – unexpected – supporting *ortho*-C–H phenyl agostic interactions occur with parent DPEphos.

Results and Discussion

Synthesis of o-F,F-DPEphos, 1-F,F

The di-*ortho*-fluorine analogue of DPEphos, *o*-F,F-DPEphos (**1-F,F**) was synthesized via addition of Li[2,6-$F_2C_6H_3$] to 2,2′-$(PCl_2)_2Ph_2O$ (Scheme 1), as previously reported for the synthesis of other substituted DPEphos ligands.[17] Aqueous workup afforded an analytically pure product as a white microcrystalline solid on recrystallization, in moderate (30%) yield, which was fully characterized by multinuclear NMR spectroscopy (CD_2Cl_2). One environment is observed in both the $^{31}P\{^1H\}$ (δ −62.5) and $^{19}F\{^1H\}$ (δ −100.7) NMR spectra, each displaying *J*(PF) coupling (40 Hz), to give a quintet and doublet respectively. The ^{31}P signal is shifted 45.9 ppm upfield compared to the parent DPEphos (δ −16.6). A similar shift is observed between PPh_3 (δ −4.7)[38] and $PPh(2,6\text{-}F_2C_6H_4)_2$ (δ −50.6).[12] The single ^{19}F environment observed suggests free rotation of the aryl group[39] as well as ether backbone flexibility that makes all of the substituted aryl groups equivalent.

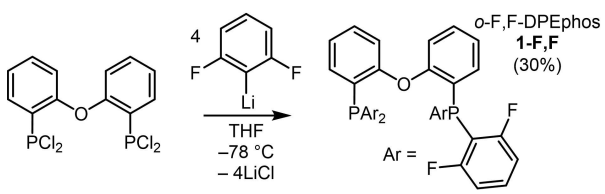

Scheme 1. Synthesis of *ortho*-F,F-DPEphos, **1-F,F**.

Synthesis, characterization and comparison of Au_2Cl_2(o-R,R-DPEphos) complexes

With the new ligand in hand its coordination chemistry with the {AuCl} fragment was investigated. Gold complexes with *ortho*-substituted aryl phosphines are well established in catalysis,[4,5] but *ortho*-substituted DPEphos variants are, to our knowledge, unknown. The corresponding Au_2Cl_2(*o*-F,F-DPEphos) complex, **2-F,F**, was synthesized using a similar method as reported for parent *o*-H,H-DPEphos,[37] **2-H,H**, by addition of two equivalents of Au(THT)Cl (THT = tetrahydrothiophene) to **1-F,F** in CH_2Cl_2 solution (Scheme 2). **2-F,F** was isolated as a white crystalline solid in a moderate yield (52%). Figure 2 shows the solid-state structure of **2-F,F**, which shows a μ^2,κ^1,κ^1-*o*-F,F-DPEphos ligand bridging two linear AuCl groups [Cl–Au–P; 175.24(5)° and 177.09(6)°]. The Au atoms are orientated in a *trans* arrangement, facilitated by a twist of the ligand backbone by 73° (arene-arene plane angle), imposing non-crystallographic, C_2 symmetry. There are no aurophilic interactions[40] [Au···Au = 6.1792(6) Å].

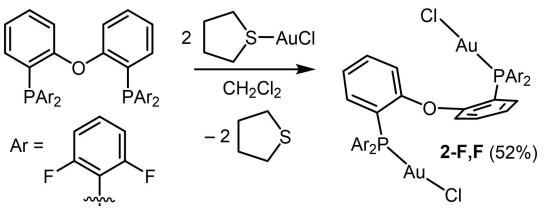

Scheme 2. Formation of Au_2Cl_2(*o*-F,F-DPEphos), **2-F,F**.

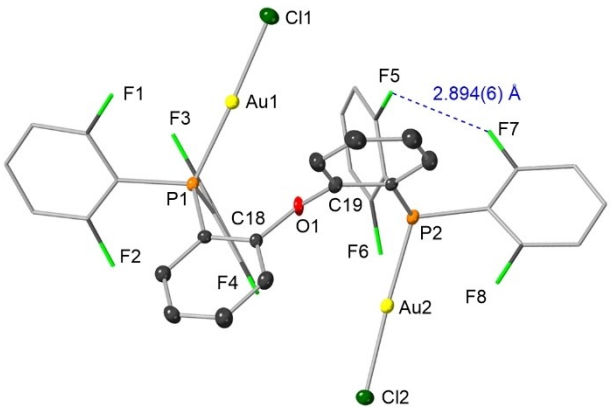

Figure 2. Crystallographically determined structure of **2-F,F**. Ellipsoids shown at the 50% probability level. Hydrogen atoms are omitted and the terminal aryl groups are modelled in stick form for clarity. Selected bond lengths (Å) and angles (°): P1–Au1, 2.225(1); Au1–Cl1, 2.276(1); P2–Au2, 2.230(1); Au2-Cl2, 2.278(1); Au1–Au2, 6.1792(6); Cl1–Au1–P1, 177.09(6); Cl2–Au2–P2, 175.24(5); C18-O1-C19, 117.8(3).

Research Article
doi.org/10.1002/ejic.202200174

This structure is in contrast with the previously reported solid-state structure of **2-H,H**, which has a much closer Au···Au contact [3.0116(4) Å], typical for an aurophilic interaction, i.e. 2.5–3.5 Å.[40] Each Au center in **2-F,F** shows a number of relatively close Au···F distances (~3.0 Å), which sit at the threshold defined for significant M···F interactions.[41] The C_2 symmetry observed in the solid-state is retained in the solution state. In the $^{31}P\{^1H\}$ NMR spectrum (CD_2Cl_2, 295 K) a single ^{31}P signal is observed at δ −23.1 as a sharp 1:2:3:2:1 apparent quintet, coupling to four equivalent ^{19}F nuclei [J(PF) = 25 Hz]. This is a large upfield shift compared to **2-H,H** (δ 21.6).[37] Two equal intensity ^{19}F environments are observed at δ −97.3 and δ −97.9 in the $^{19}F\{^1H\}$ NMR spectrum as doublets of triplets, both coupling to one ^{31}P [J(PF) = 25 Hz] and two ^{19}F nuclei, J(FF) (7 Hz) – the latter confirmed by a ^{19}F-COSY experiment. These are not particularly shifted from free ligand (δ −100.7). A total of eight aromatic environments were observed for **2-F,F** in the ^1H NMR spectrum, assigned to the diphenylether backbone and two sets of *meta*-H and *para*-H environments. These data suggest a rapid rotation of the 2,6-$F_2C_6H_3$ groups around the P–C bond, but that inversion of the diphenyl backbone does not occur, or is very slow on the NMR timescale, leading to two different aryl groups. We suggest the ^{19}F-^{19}F coupling observed is due to through space coupling,[42,43] for which a dependence on the F···F distance has been investigated computationally by Mallory and co-workers.[44] A F···F distance of 3.0 Å would be expected to give a J(FF) of ~7 Hz.[45] This is consistent with that measured for the closest F···F distance (F5···F7) on adjacent aryl groups of 2.894(6) Å in **2-F,F**, and the observed coupling constant. These interactions would be time-averaged in solution leading to the observed symmetry in solution.

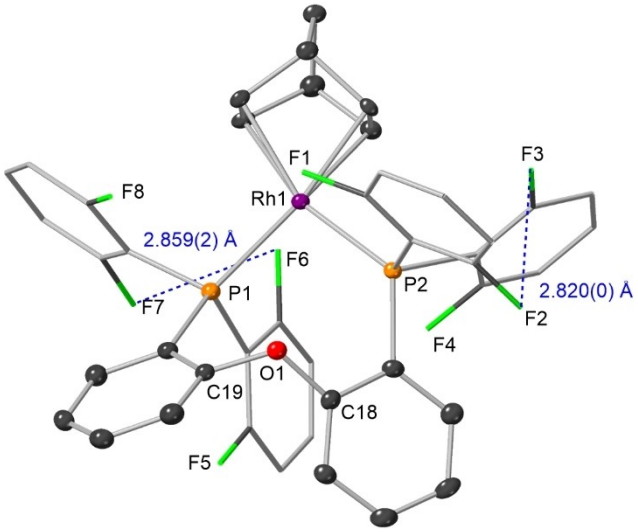

Figure 3. Crystallographically determined structure of **3-F,F**. Ellipsoids shown at the 50% probability level. Hydrogen atoms and $[BAr^F_4]^-$ anion omitted and substituted aryl groups in stick form for clarity. Selected bond lengths (Å) and angles (°): Rh1-P1, 2.3180(6); Rh1-P2, (2.3757(6); Rh1-O1, 3.480(2); Rh1-F1, 2.876(2); Rh1-F6, 3.147(2); P1-Rh1-P2, 101.48(2); C18-O1-C19, 116.8(2).

Synthesis, characterization and structural behavior of [Rh(o-F,F-DPEphos)(NBD)][BAr$^F_4$], 3-F,F

[Rh(*o*-F,F-DPEphos)(NBD)][BAr^F_4], **3-F,F**, was synthesized via addition of **1-F,F** to [$Rh(NBD)_2$][BAr^F_4] in a 1,2-$F_2C_6H_4$ solution using a similar synthetic procedure to that previously used for the synthesis of [Rh(*o*-H,^{i}Pr-DPEphos)(NBD)][BAr^F_4] (Scheme 3).[17] An analytically pure orange microcrystalline powder was obtained in a good yield (77%). A small number of crystals suitable for analysis by x-ray diffraction were obtained from slow diffusion of pentane into a THF solution of **3-F,F**. The resulting solid-state structure of **3-F,F**, Figure 3, shows the diphosphine bound in a *cis*-κ^2-P,P arrangement, with no oxygen coordination [Rh···O 3.480(2) Å]. With the η^2,η^2 bound NBD ligand there is an overall pseudo-square planar geometry for the cation. Rh–P bond distances of 2.3180(6) Å and 2.3757(6) Å are typical of such Rh(I) complexes.[17] The ether-oxygen atom sits just off the square plane, in an envelope-like[46] conformation, as previously observed in [Rh(*o*-H,H-DPEphos)(NBD)][BAr^F_4] (**3-H,H**).[17] While this gives the complex overall crystallographic C_1 symmetry, in solution a low energy ring inversion of the diphenyl ether backbone would lead to the observed time-averaged C_2 symmetry. Relatively close F···F distances are present [F2···F3 = 2.820(0) Å, F6···F7 = 2.859(2) Å]. In the room temperature ^{31}P NMR spectrum of **3-F,F**, a single doublet was observed at δ −17.3 [J(RhP) = 162 Hz] with no observable coupling to fluorine, unlike for **2-F,F**. Very broad signals centered at δ −90.9, −97.7 and −102.5, in the ratio 1:2:1, were observed in the ^{19}F NMR spectrum, in addition to the signal due to $[BAr^F_4]^-$. In the ^1H NMR spectrum, three NBD environments observed in a 4:2:2 ratio suggests time averaged C_{2V} symmetry in solution. On cooling to 183 K in CD_2Cl_2 the integral 4H alkene signal resolves into two separate, integral 2H, signals. The ^{31}P NMR spectrum is essentially unchanged on cooling apart from the doublet being broadened (fwhm = 275 Hz) that may suggest unresolved coupling to ^{19}F. In the ^{19}F NMR spectrum at 183 K, four ^{19}F signals were observed, in a 2:2:2:2 ratio at δ −90.8, −97.5, −98.1 and −103.5. Only one of these (δ −98.1) is resolved into a doublet [J(PF) = 38 Hz] which is consistent with the broadening of the ^{31}P NMR signal at this temperature. Similar behavior with regard to selective J(PF) coupling has been reported in *trans*-$PtCl_2(PEt_3)(P(2,6\text{-}F_2C_6H_3)_3$, in which only one pair of ^{19}F nuclei couple to ^{31}P, J(PF) = 30 Hz.[12] No ^{103}Rh-^{19}F coupling is observed in **3-F,F**. Warming to 318 K, results in a single very broad signal being observed in the $^{19}F\{^1H\}$ NMR spectrum, centered at δ −98.1. The aromatic signals in the ^1H NMR spectrum are overlapping, even at 183 K, and therefore

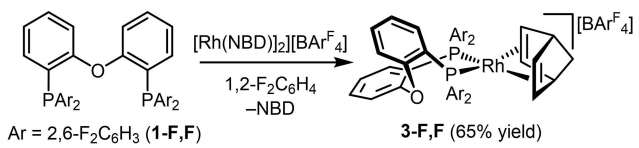

Scheme 3. Preparation of [Rh(*o*-F,F-DPEphos)(NBD)][BAr^F_4] **3-F,F**.

Research Article
doi.org/10.1002/ejic.202200174

not helpful for structural elucidation. Combined, these data suggest a low energy ring flipping process combined with restricted rotation of the fluorinated aryl groups[12,13] are occurring, giving the complex overall C_2 symmetry at low temperature, with four distinct ^{19}F environments. We suggest this backbone flipping attenuates through space F···F couplings, despite the reasonably close contacts being observed in the solid-state. This is in contrast to **2-F,F** where F···F coupling is observed but inversion of the diphenyl ether unit does not occur. Ring-flipping processes have been reported previously in POP-type ligands,[47,48] and most relevantly, a similar dynamic process was reported in **3-H,H**.[17] Interestingly, in the solid-state structure of **3-F,F**, there is a fluorine atom located in the apical position of the pseudo square planar Rh(I) center, with relatively close Rh···F distance: F1···Rh1 = 2.876(2), Figure 4. Similar close metal-fluorine contacts [M···F = 3.0997(8), 3.074(1) Å] were reported by Togni et al. for [MCl(COD)(diphenyl(5,6,7,8-tetrafluoronapthalen-1yl)] (M=Rh or Ir, COD = cyclooctadiene), for which ^{19}F-^{31}P coupling constants of 62 and 75 Hz (Ir and Rh respectively) were also measured. For these complexes it is also interesting to note that the fluorine atom in close contact with the metal is shifted ~20 ppm downfield compared to the other signals in the ^{19}F NMR spectrum.[49] In solution for **3-F,F** these interactions are likely to be time averaged, between F1···Rh1 and F6···Rh1, given the C_2 symmetry and restricted rotation observed. No *J*(RhF) was observed, although this is likely to be small (< 10 Hz).[49] Geometrically related anagostic[36,50] Rh···H–C interactions are observed in complex **3-H,H** (Figure 4),[17] expressed by downfield chemical shifts in the ^1H NMR spectrum for the C–H groups involved. Such interactions are geometrically enforced, with the spatial orientation of the C–H bonds perpendicular to the Rh-square plane leading to ring-current induced chemical shift changes. While we have been unable to definitively assign a particular ^{19}F chemical shift to the close Rh···F interactions in **3-F,F** it is tempting to suggest that the signal at δ −98.1 that shows the coupling to ^{31}P [*J*(PF) = 30 Hz] is due to the F1/F6 pair via coupling through the Rh-center. However, this signal is not particularly shifted from free ligand (δ −100.7), whereas there is a signal upfield shifted by ~10 ppm at δ −90.8. More detailed computational studies are needed to reconcile these chemical shift differences with the observed structure.

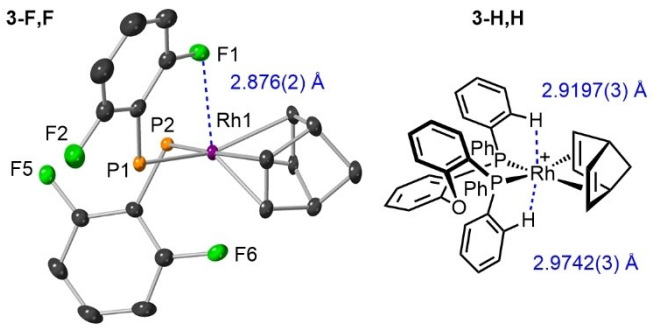

Figure 4. Truncated solid-state structure of **3-F,F** and diagramed structure of the cationic portion of **3-H,H**[17] highlighting the close Rh···F and Rh···H contacts respectively. Ellipsoids at the 50% probability level. $[BAr^F_4]^-$, hydrogen atoms and aryl groups not involved in Rh···F contacts are removed for clarity.

Hydrogenation products of 3-H,H and 3-F,F

Schrock-Osborn [Rh(chelating-phosphine)(NBD)]$^+$ systems are popular precatalysts for a variety of transformations, for example in olefin hydrogenation and hydroacylation reactions.[1,35] They are typically activated by hydrogenation of the diene moiety to form Rh(I) solvated[25,51] or Rh(III) dihydride containing complexes.[52,53] Hydrogenation of [Rh(*o*-H,H-DPEphos)(NBD)][BAr^F_4] in the presence of coordinating solvents, such as *o*-xylene, acetone and C_6H_5F have previously been shown to form Rh(I) solvated complexes: [Rh(*o*-H,H-DPEphos)(η^6-*o*-xylene)][BAr^F_4],[28] [Rh(*o*-H,H-DPEphos)(acetone)$_2$][BAr^F_4],[24,25] and [Rh(*o*-H,H-DPEphos)(η^6-C_6H_5F)][BAr^F_4][26] respectively, the last two characterised in-situ. With the bulkier, *ortho*-methyl substituted DPEphos ligand a dihydride Rh(III) complex forms, [Rh(*o*-Me-DPEphos)H$_2$(acetone)][BAr^F_4], whereas with *ortho*-^{i}Pr a C–H activated product results.[17] Here, we contrast the activation products of **3-H,H** and **3-F,F** after treatment with H_2 in the less coordinating[54,55] solvent, 1,2-$F_2C_6H_4$ (Scheme 4). An atmosphere of 1 bar H_2 was applied to a 1,2-$F_2C_6H_4$ solution of **3-H,H** and a color change from orange to dark red was observed after several minutes.

After 20 minutes, in-situ $^{31}P\{^1H\}$ NMR spectroscopy indicated that all of the **3-H,H** had reacted, and two new ^{31}P signals were observed (δ 42.9 and δ 36.2) alongside free norbornane in the ^1H NMR spectrum. The resulting organometallic product, **4-H,H**, was isolated as a purple solid and characterized using NMR spectroscopy and ESI-MS. Unfortunately, crystals suitable for x-ray diffraction could not be obtained, despite repeated attempts. In the ^{31}P NMR spectrum of this isolated product, two broad signals at δ 43.3 and δ 36.5 are observed as a doublet [*J*(RhP) = 174 Hz] and a doublet of doublets [*J*(RhP) = 154 Hz, *J*(PH) = 74 Hz] respectively at a very similar chemical shift to the

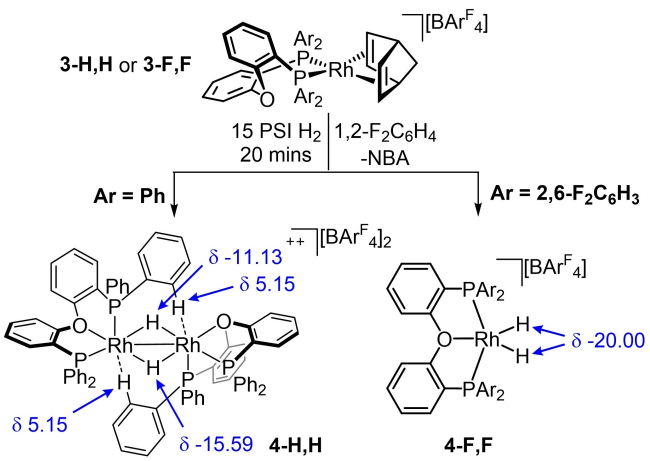

Scheme 4. Formation of **4-H,H** and **4-F,F** from the hydrogenation of **3-H,H** and **3-F,F** in 1,2-$F_2C_6H_4$.

in situ prepared complex. The large measured *J*(PH) coupling suggests a *trans*-PH arrangement.[56] Upon ^{1}H-decoupling, the signal at δ 43.3 sharpens to a doublet of doublets [*J*(RhP) = 174 Hz, *J*(PP) = 26 Hz]. The signal at δ 36.5 resolves into a complex second order multiplet on ^{1}H decoupling.[57] These signals were shown to couple to one another via ^{31}P-^{31}P-COSY NMR experiments. In the ^{1}H NMR spectrum of **4-H,H**, two hydride signals at δ −11.13 and δ −15.59 are observed as complex multiplets (Figure 5), integrating in the ratio 1:1:2 relative to the $[BAr^{F}_{4}]^{-}$ anion. These data are suggestive of a dimer with bridging hydrides, i.e. $[Rh_2(DPEphos)_2(\mu\text{-}H)_2][BAr^{F}_{4}]_2$. Spin simulation of a AA'MM'NN'XX' coupling systems (Figure 5) for the hydride resonances revealed the hydride signal at δ −11.13 is coupling to two of each of the following: Rh [*J*(RhH) = 20 Hz], *trans*-P [*J*(PH) = 74 Hz], *cis*-P [*J*(PH) = 17 Hz] and very small *cis*-hydride/hydride coupling [*J*(HH) ≈ 2 Hz]. The signal at δ −15.59 also couples to two Rh, and two sets of two ^{31}P nuclei [*J*(RhH) = 34 Hz], *cis*-P [*J*(PH) = 5 Hz], *cis*-P [*J*(PH) = 9 Hz] and a corresponding small hydride/hydride coupling [*J*(HH) ≈ 2 Hz]. In decoupling ^{31}P both hydride signals collapse to triplets [*J*(RhH) = 20 Hz and 34 Hz respectively]. These data suggest both hydrides are bridging two Rh atoms, with one *trans* to a ^{31}P atom.

An upfield shifted aromatic signal is also observed at δ 5.15 of relative integral 2H. This signal has doublet of doublet multiplicity [*J*(HH) = 8 Hz and *J*(PH) = 4 Hz], which collapses to a doublet [*J*(HH) = 8 Hz] upon ^{31}P-decoupling, and is shifted 2.1 ppm upfield compared to the *ortho*-phenyl signal in free *o*-H,H-DPEphos in CD_2Cl_2.[17] A similar upfield shifted signal (δ 3.94, integral 2H) was reported in the crystallographically characterized dimer $[Rh_2(\sigma,\mu\text{-}CH\text{-}\kappa^2\text{-}P,P\text{-}o\text{-}H,H\text{-}DPEphos)_2(\sigma,\mu\text{-}H_2B)_2NHMe)][Al(OC(CF_3)_3)_4]$,[27] in which an *ortho*-phenyl C–H bond of DPEphos coordinates via an agostic bond to the neighboring Rh-center.[27] When **4-H,H** was analyzed by anerobic ESI-MS[58] only $[Rh(DPEphos)]^{+}$ (m/z = 641.2, calc. 641.1) and $[Rh(o\text{-}H,H\text{-}DPEphos)]_2^{2+}$ (641.2 m/z, isotopologues increasing in m/z = 0.5) were observed due to facile H_2 loss and dimer fragmentation. In contrast, when D_2 was used to activate **3-H,H**, forming $[Rh(o\text{-}H,H\text{-}DPEphos)(\mu\text{-}D)]_2[BAr^{F}_{4}]_2$ ***d*$_2$-4-H,H** the deuteride $[Rh(o\text{-}H,H\text{-}DPEphos)(\mu\text{-}D)]_2^{2+}$ was also observed in the ESI-MS spectrum (m/z = 643.2, calc. 643.1). This is likely a consequence of D_2 being lost less easily than H_2 under ESI-MS conditions.[59,60] Combined, these NMR and mass spectrometric data allow a dicationic dimeric structure to be proposed for **4-H,H**, which has two different bridging hydrides and a bridging σ-CH agostic interaction: $[Rh(H)(fac\text{-}\kappa^3\text{-}P,O,P\text{-}\mu\text{-}CH\text{-}DPEphos)]_2[BAr^{F}_{4}]_2$ (Scheme 4). Without a solid-state structure we cannot determine if the ether-linkage in the DPEphos backbone is coordinated or not. Both motifs are known for *cis*-PP-DPEphos complexes.[19] We favor a κ^3-P,O,P coordination mode with a Rh–Rh bond on the basis of a 34 cluster valence electron count for the dimer.[61] Related dimeric complexes have previously been reported in $[Rh_2(o\text{-}H,H\text{-}DPEphos)_2(\mu\text{-}H)(\mu\text{-}(H_2B{=}NHMe)][BAr^{F}_{4}]$,[27] $Rh_2(H)(\mu\text{-}H)_3(o\text{-}H,H\text{-}DPEphos)_2$,[26,27] and $[Ir(\kappa^3\text{-}P,O,P\text{-}Xantphos)(H)(\mu\text{-}H)]_2[BAr^{F}_{4}]_2$ (Xantphos = 4,5-bis(diphenylphosphino)-9,9-dimethylxanthene).[62]

When the same H_2 activation process was employed with **3-F,F** a monomeric complex is formed. Addition of H_2 to **3-F,F** in 1,2-$F_2C_6H_4$ solvent resulted in a color change from orange to yellow, rather than the dark red of **4-H,H**. The resulting complex was characterized by in-situ NMR spectroscopy. In contrast to **4-H,H** a single ^{31}P environment was observed in the $^{31}P\{^{1}H\}$ spectrum at δ −6.7 [*J*(RhP) = 130 Hz], with a reduced magnitude *J*(RhP) than measured in **3-H,H** [*J*(RhP) = 162 Hz] suggestive of a Rh(III) complex with a *trans*-P,P arrangement.[19] A single hydride resonance, of relative integral 2H, was observed at δ −20.00 as a doublet of triplets [*J*(RhH) = 34 Hz, *J*(PH) = 17] that collapses to a doublet upon ^{31}P-decoupling. A single environment is observed in the ^{19}F NMR spectrum, very close to free ligand, δ −100.9, with no coupling to ^{31}P seen. These data allow us to assign this complex as five-coordinate $[Rh^{III}(mer\text{-}\kappa^3\text{-}P,O,P\text{-}o\text{-}F,F\text{-}DPEphos)H_2][BAr^{F}_{4}]$, **4-F,F** (Scheme 4). Degassing the sample of **4-F,F** resulted in decomposition to multiple products, likely due to loss of H_2, and therefore **4-F,F** could not be isolated. Consistent with facile H_2 loss, ESI-MS analysis showed a single species at m/z = 785.0, corresponding to $[Rh(o\text{-}F,F\text{-}DPEphos)]^{+}$ (calc. m/z = 785.0). Closely related complexes to **4-F,F** have been reported $[Rh(mer\text{-}\kappa^3\text{-}P,O,P\text{-}Xantphos)H_2][BAr^{F}_{4}]$[53,63] and $[Rh(o\text{-}Me\text{-}DPEphos)H_2(acetone)][BAr^{F}_{4}]$.[17,64] We currently can only speculate on the mechanism of formation of dimeric **4-H,H**, and thus why *ortho*-F substitution provides a different, monomeric product for **4-F,F**. However that **4-H,H** is suggested to have a bridging Rh···H–C agostic interaction, and that equivalent M···F–C interactions are less common,[49] dimer formation through partial H_2 loss may be stabilized with the parent DPEphos ligand whereas no such stabilization is possible for **4-F,F** and decomposition occurs.

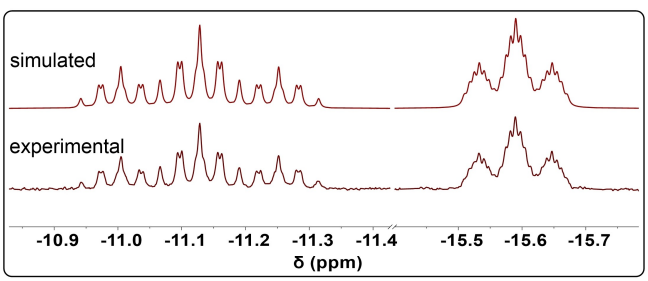

Figure 5. The experimental and spin-simulated AA'MM'NN'XX' coupling pattern in the hydride signal of **4-H,H** (600 MHz, 298 K, CD_2Cl_2).

Conclusion

We have highlighted the impact of *ortho*-fluorine substitution in organometallic chemistry through the control of aurophilic interactions in $Au_2Cl_2(o\text{-}R,R\text{-}DPEphos)$ complexes (R=H or F) and the different hydrogenation products of common Schrock-Osborn precatalysts. In the process, we have characterized an unexpected dimeric complex with the parent *o*-H,H-DPEphos ligand which has a bridging C–H···Rh agostic interaction.

Experimental Section

All experiments were performed under an atmosphere of argon, using standard Schlenk techniques on a dual vacuum/inlet manifold unless specified otherwise. Glassware was dried in an oven at 140 °C overnight or flame dried under vacuum prior to use. Pentane, hexane, THF, diethyl ether and CH_2Cl_2 were dried using an Mbraun SPS-800 solvent purification system and degassed by three freeze-pump-thaw cycles. 1,2-$F_2C_6H_4$ was stirred over Al_2O_3 for two hours and then CaH_2 overnight before vacuum transfer and subsequent degassing by three freeze-pump-thaw cycles. Dichloromethane-D_2 (CD_2Cl_2) was dried overnight with CaH_2 before vacuum transfer and subsequent degassing by three freeze-pump-thaw cycles and storage over 3 Å molecular sieves. [Rh(NBD)$_2$][BAr^F_4] was prepared via the literature procedure.[65] All other reagents, were purchased from commercial vendors and used as received. NMR data was collected on either a Bruker 500 MHz AVC or Bruker AVIII 600 MHz widebore spectrometer. Residual protio solvent resonances were used as a reference for ^{1}H NMR spectra.^{31}P and ^{11}B NMR spectra were referenced externally to 85% H_3PO_4 and $F_3B{\cdot}OEt_2$ respectively. All chemical shifts (δ) are quoted in ppm and coupling constants in Hz. Aerobic electrospray ionization mass spectrometry (ESI-MS) was carried out using a Bruker compact® time of flight mass spectrometer by Mr. Karl Heaton at the University of York for compounds **1-F,F**, **2-F,F** and **3-F,F**. Air sensitive mass spectrometry, using a bespoke N_2 filled glovebox connected to a Bruker ESI-ion trap spectrometer[58] was used for analysis of **4-H,H** and **4-F,F**. Elemental analyses were conducted by Dr. Graeme McAllister at the University of York.

***o*-F,F-DPEphos 1-F,F**: Synthesis of 2,2′-(PCl_2)$_2$$Ph_2O$ (Scheme 1) was done in accordance with literature procedures.[16,30] In a separate J. Young's ampoule, N,N,N′,N′-tetramethylenediamine (0.42 ml, 2.8 mmol, 4.3 equiv.) was added dropwise to ^{n}BuLi (1.07 ml, 2.4 M solution in hexanes, 2.6 mmol, 4 equiv.) at 0 °C. The mixture was cooled to −78 °C and THF (2 ml) followed by 2,6-difluorobromobenzene (0.29 ml, 2.6 mmol, 4 equivalents) were added dropwise and the mixture was left to stir for 1 hour at −78 °C. The previously prepared 2,2′-(PCl_2)$_2$$Ph_2O$ (200 mg, 0.54 mmol, 1 equiv.) in 4 ml of THF was cooled to −78 °C and the aryl lithium was added dropwise, keeping both solutions at −78 °C. The resulting orange mixture was allowed to warm to room temperature, then stirred for 30 minutes and checked by ^{19}F and ^{31}P NMR spectroscopy for completion. The mixture was then cooled to 0 °C, quenched with methanol (1 ml) and saturated ammonium chloride solution (10 ml). The now air stable product was extracted with ethyl acetate (3×10 ml), dried over Na_2SO_4, filtered, and washed with cold pentane yielding the product as a white solid. Recrystallisation with pentane and CH_2Cl_2 yielded **1-F,F** as a white microcrystalline solid (109 mg, 30%): ^{31}P{^{1}H} NMR (202 MHz, CD_2Cl_2, 295 K): δ −62.5 (quint, J_{FP} = 40 Hz). ^{19}F NMR (471 MHz, CD_2Cl_2, 295 K): δ −100.7 (d, J_{PF} = 40 Hz). ^{1}H NMR (500 MHz, CD_2Cl_2, 295 K): δ 7.33 (tt, J = 8 Hz and 6 Hz, 4H, Ar), 7.26 (m, J = 8 and 2 Hz, 2H, Ar), 7.06 (dd, J = 7 and J_{PH} = 4 Hz, 2H, Ar), 7.00 (dd, J = 8 and 7 Hz, 2H, Ar), 6.82 (dt, J = 8 and 2 Hz, 8H, *meta-H* on substituted phenyl), 6.74 (dd, J_{HH} = 8 and J_{PH} = 5 Hz, 2H, *ortho*-H on backbone). ^{13}C{^{1}H} NMR (126 MHz, CD_2Cl_2, 295 K): δ 165.6–163.6 (dt, J_{CF} = 250 and J_{CP} = 9 Hz, Ar), 158.9 (s, Ar), 158.5 (s, Ar), 132.2 (s, Ar), 132.0 (t, J = 11 Hz), 130.4 (d, J = 1 Hz Ar), 123.5 (s, Ar), 117.4 (s, Ar), 111.6 (d, J = 5 Hz, Ar), 111.4 (dd, J = 5 Hz, J = 1 Hz, Ar). ESI-MS (CH_2Cl_2): *m/z* [M + H]$^+$ 683.0942 (calc. 683.0934) with the correct isotope pattern. Elemental analysis found (calc. for $C_{36}H_{20}F_8OP_2$): C 63.38 (63.35) H 3.19 (2.95).

Au_2Cl_2(*o*-F,F-DPEphos) 2-F,F: A solution of **1-F,F** (1.05 equiv.) in CH_2Cl_2 (2 ml) was added dropwise to a CH_2Cl_2 (2 ml) solution of Au(THT)Cl (2 equiv.),[66] and left to stir for one hour, leaving a colorless solution. The solvent was mostly removed *in vacuo* before pentane (10 ml) was added, precipitating out a white solid. The precipitate was the filtered and washed with further pentane (4× 5 ml) and dried under Schlenk line vacuum overnight (< 1× 10^{-1} mbar) leaving a white powder (both white powders) that was transferred into an argon glovebox for storage. Colorless crystals suitable for x-ray diffraction were obtained by slow diffusion of pentane into a CH_2Cl_2 solution of **2-F,F** (26 mg, 52%): ^{31}P{^{1}H} NMR (202 MHz, CD_2Cl_2, 295 K): δ −23.1 (app. quint., J_{FP} = 25 Hz). ^{19}F NMR (471 MHz, CD_2Cl_2, 295 K): δ −97.3 (dt, J_{PF} = 25 Hz, J_{FF} = 7 Hz), −97.9 (dt, J_{PF} = 25 Hz, J_{FF} = 7 Hz). ^{1}H NMR (500 MHz, CD_2Cl_2, 295 K): δ 7.60 (m, 2H, Ar), 7.56 (dd, J = 7 Hz, 2H, Ar), 7.44 (m, 2H, Ar), 7.27 (dd, J = 7 Hz, 2H, Ar), 7.22 (m, 2H, Ar), 7.06-6.99 (m, 6H {2 + 4 coincidence}, Ar), 6.82 (ddd, J = 9 and 4 Hz, 4H, Ar). ESI-MS (CH_2Cl_2): *m/z* [M−Cl]$^+$ 1110.9852 (calc. 1110.9881) with correct the isotope pattern. Multiple samples were submitted for elemental analysis, but no results were within 0.4% of the theoretical percentage mass by weight for carbon or hydrogen. Persistent pentane may be the cause of the inconsistent elemental analysis (see ^{1}H NMR spectrum in the ESI).

[Rh(*o*-F,F-DPEphos)(NBD)][BAr^F_4] 3-F,F: 1,2-$F_2C_6H_4$ (10 ml) was added to [Rh(NBD)$_2$][BAr^F_4] (63 mg, 0.055 mmol, 1 equiv.)[65,67] and **1-F,F** (38 mg, 0.055 mmol, 1 equiv.) in a J. Young's Ampoule to form an orange solution. The mixture was stirred for two hours at room temperature. The solvent was removed *in vacuo* to leave a purple oil which was triturated with pentane to give a red solid. The solid was filtered and washed with further pentane (3×5 ml) and dried under Schlenk line vacuum (< 1×10^{-1} mbar) overnight, leaving **3-F,F** as an orange microcrystalline powder (73 mg, 77%,): ^{31}P{^{1}H} NMR (202 MHz, CD_2Cl_2, 295 K): δ −17.4 (d, J_{RhP} = 163 Hz). ^{1}H NMR (500 MHz, CD_2Cl_2, 295 K): δ 7.72 (s, 8H, *o*-CH, BAr^F_4), 7.55 (s, 4H, *p*-CH, BAr^F_4), 7.51 (br m, 4H, Ar), 7.40 (m, J = 9 Hz and 2 Hz, 4H, Ar), 7.13–6.83 (complex multiplet, 12H, Ar), 4.16 (s, 4H, sp^2-C*H* NBD), 3.80 (s, 2H, sp^3-C*H* NBD), 1.44 (s, 2H, CH_2 NBD). ^{1}H NMR (500 MHz, CD_2Cl_2, 318 K) selected data: δ 7.73 (s, 8H, *o*-CH, BAr^F_4), 7.55 (s, 4H, *p*-CH, BAr^F_4), 4.18 (s, 4H, sp^2-C*H* NBD), 3.81 (s, 2H, sp^3-C*H* NBD), 1.45 (s, 2H, CH_2 NBD). ^{1}H NMR (500 MHz, CD_2Cl_2, 183 K): δ 7.72 (s, 8H, *o*-CH, BAr^F_4), 7.57 (m, 4H, Ar), 7.51 (s, 4H, *p*-CH, BAr^F_4), 7.37 (m, 4H, Ar), 7.11 (t, J = 9 Hz, 2H, Ar), 7.07–6.93 (br m, 8H, Ar), 6.49 (t, J = 9 Hz, 2H, Ar), 4.23 (s, 2H, sp^2-C*H* NBD), 3.87 (s, 2H, sp^2-C*H* NBD), 3.74 (s, 2H, sp^3-C*H* NBD), 1.35 (s, 2H, CH_2 NBD). ^{19}F NMR (471 MHz, CD_2Cl_2, 295 K): δ −62.9 (s, 24F, BAr^F_4), −88.9 to −92.5 (br s, 2F), −95.2 to −100.2 (br s, 4F), −100.6 to 104.5 (br s, 2F). ^{19}F NMR (471 MHz, CD_2Cl_2, 183 K) selected data: δ −90.8 (s, 2F), −97.9 (s, 2F), −98.1 (br d, J = 38 Hz, 2F), −103.5 (s, 2F). ^{19}F NMR (471 MHz, CD_2Cl_2, 318 K) selected data: δ −98.1 (br s, 8F). ESI-MS (1,2-$F_2C_6H_4$): *m/z* [M]$^+$ 877.0557 (calc. 877.0543) with correct isotope pattern. Elemental analysis found (calc. for $C_{75}H_{40}BF_{32}OP_2Rh$): C 51.74 (51.75) H 2.40 (2.32).

[Rh(*o*-H,H-DPEphos)(μ-H)$_2$]$_2$[BAr^F_4] 4-H,H: A sample of [Rh(*o*-H,H-DPEphos)(NBD)][BAr^F_4] **2-H,H** (40 mg, 0.025 mmol) was dissolved in 1–2-$F_2C_6H_4$ (0.5 ml) in a high pressure J. Youngs NMR tube. The atmosphere was removed by three successive freeze-pump-thaws and the NMR tube was placed under an atmosphere of 15 PSI H_2 and successively rotated for ten minutes which formed a dark red solution. The 1–2-$F_2C_6H_4$ solution was transferred to a Youngs Flask equipped with a stirrer bar. Pentane (5 ml) was added to the solution with vigorous stirring and a purple solid precipitated. The solvent was removed by filter cannula and the purple solid was washed with pentane twice more (5 ml) before drying under Schlenk line vacuum (< 1×10^{-1} mbar) for two hours (30 mg, 0.010 mmol, 80%): ^{31}P{^{1}H} NMR (243 MHz, CD_2Cl_2, 298 K): δ 43.3 (dd, J_{RhP} = 174 Hz and J_{PP} = 26 Hz), 36.5 (complex 2nd order multiplet). ^{31}P NMR (243 MHz, CD_2Cl_2, 298 K): δ 43.3 (br d, J_{RhP} = 174 Hz), 36.5 (br dd, J_{RhP} = 154 Hz, J_{PH} = 74 Hz). ^{1}H NMR (600 MHz, CD_2Cl_2, 298 K) δ 7.23 (s, 16H, *ortho*-H BAr^F_4), 7.60–7.50 (m, 6H, Ar), 7.55 (s, 8H, *para*-H BAr^F_4), 7.47 (m, 3H, Ar) 7.48 7.44–7.37 (m, 6H, Ar), 7.34–7.20 (m, 14H,

Ar), 7.14 (dd, $J=6$ Hz, 3H, Ar), 7.12–7.04 (m, 5H, Ar), 6.97 (dd, $J=8$ and 12 Hz, 4H, Ar), 6.84–6.78 (m, 6H, Ar), 6.68 (dd, $J=7$ Hz, 2H, Ar), 5.15 (dd, $J_{PH}=4$ and $J_{HH}=8$ Hz, 2H, CH σ-agostic), −11.13 (complex multiplet, $J_{PH(trans)}=74$ Hz, $J_{PH(cis)}=17$ Hz, $J_{RhH}=20$ Hz, 1H, bridging hydride *trans* to ^{31}P) and −15.59 (complex multiplet, $J_{RhH}=34$ Hz, $J_{PH(cis)}=5$ Hz, $J_{PH(cis)}=9$ Hz, 1H, bridging hydride *trans* to CH σ-agostic). ^{1}H NMR (600 MHz, CD_2Cl_2, 298 K) selected data: δ −11.13 (triplet, $J_{RhH}=20$ Hz, 1H, bridging hydride *trans* to ^{31}P), −15.59 (triplet, $J_{RhH}=34$ Hz, 1H, bridging hydride *trans* to CH σ-agostic).

In-situ characterization of [Rh(*o*-F,F-DPEphos)(H)$_2$][BAr$^F{}_4$] **4-F,F**: A sample of [Rh(*o*-F,F-DPEphos)(NBD)][BAr$^F{}_4$] **3-F,F** (40 mg, 0.023 mmol) was dissolved in 1–2-$F_2C_6H_4$ (0.5 ml) in a high pressure J. Youngs NMR tube. The atmosphere was removed by three successive freeze-pump-thaws and the NMR tube was placed under an atmosphere of 15 PSI H_2 and successively rotated for ten minutes which formed a yellow solution. **4-F,F** was characterised in-situ by multinuclear NMR spectroscopy: ^{31}P{^{1}H} NMR (243 MHz, 1,2-$F_2C_6H_4$, 298 K): δ −6.7 (d, $J_{RhP}=130$ Hz). ^{19}F NMR (565 MHz, 1,2-$F_2C_6H_4$, 298 K): −100.9 (s, 2,6-$F_2C_6H_3$). ^{1}H NMR (600 MHz, 1,2-$F_2C_6H_4$, 298 K) selected data: δ −20.0 (dt, $J_{PH}=17$ Hz, $J_{RhH}=34$ Hz, 2H, Rh–H). ^{1}H NMR (600 MHz, 1,2-$F_2C_6H_4$, 298 K) selected data: δ −20.00 (d, $J_{RhH}=34$ Hz). Removal of the hydrogen atmosphere resulted in decomposition of **4-F,F**.

Deposition Numbers 2160287 (for **2-F,F**) and 2160288 (for **3-F,F**) contain the supplementary crystallographic data for this paper. These data are provided free of charge by the joint Cambridge Crystallographic Data Center and Fachinformationszentrum Karlsruhe Access Structures service www.ccdc.cam.ac.uk/structures.

Acknowledgements

The EPSRC for funding (ASW: EP/M024210, JJR and TMB PhD studentships through the Doctoral Training Partnership).

Conflict of Interest

The authors declare no conflict of interest.

Data Availability Statement

The data that support the findings of this study are available in the supplementary material of this article.

Keywords: Agostic · DPEphos · Gold · Phosphine · Rhodium

[1] J. F. Hartwig, *Organotransition Metal Chemistry. From Bonding to Catalysis.* University Science Books, Sausalito, **2010**.
[2] R. H. Crabtree, *The Organometallic Chemistry of the Transition Metals.* Sixth ed. Wiley, New Jersey, **2014**.
[3] L. Lavanant, A.-S. Rodrigues, E. Kirillov, J.-F. Carpentier, R. F. Jordan, *Organometallics* **2008**, *27*, 2107–2117.
[4] R. Ebule, S. Liang, G. B. Hammond, B. Xu, *ACS Catal.* **2017**, *7*, 6798–6801.
[5] D. Malhotra, M. S. Mashuta, G. B. Hammond, B. Xu, *Angew. Chem. Int. Ed.* **2014**, *53*, 4456–4459; *Angew. Chem.* **2014**, *126*, 4545–4548.
[6] J. N. L. Dennett, A. L. Gillon, K. Heslop, D. J. Hyett, J. S. Fleming, C. E. Lloyd-Jones, A. G. Orpen, P. G. Pringle, D. F. Wass, J. N. Scutt, R. H. Weatherhead, *Organometallics* **2004**, *23*, 6077–6079.
[7] C. González-Rodríguez, R. J. Pawley, A. B. Chaplin, A. L. Thompson, A. S. Weller, M. C. Willis, *Angew. Chem. Int. Ed.* **2011**, *50*, 5134–5138; *Angew. Chem.* **2011**, *123*, 5240–5244.
[8] B. D. Vineyard, W. S. Knowles, M. J. Sabacky, G. L. Bachman, D. J. Weinkauff, *J. Am. Chem. Soc.* **1977**, *98*, 5946–5952.
[9] N. A. Cooley, S. M. Green, D. F. Wass, K. Heslop, A. G. Orpen, P. G. Pringle, *Organometallics* **2001**, *20*, 4769–4771.
[10] S. J. Dossett, A. Gillon, A. G. Orpen, J. S. Fleming, P. G. Pringle, D. F. Wass, M. D. Jones, *Chem. Commun.* **2001**, 699–700.
[11] J. Fawcett, S. Friedrichs, J. H. Holloway, E. G. Hope, V. Mckee, M. Nieuwenhuyzen, D. R. Russell, G. C. Saunders, *J. Chem. Soc. Dalton Trans.* **1998**, 1477–1484.
[12] C. Corcoran, J. Fawcett, S. Friedrichs, J. H. Holloway, E. G. Hope, D. R. Russell, G. C. Saunders, A. M. Stuart, *J. Chem. Soc. Dalton Trans.* **2000**, 161–172.
[13] T. Korenaga, K. Abe, A. Ko, R. Maenishi, T. Sakai, *Organometallics* **2010**, *29*, 4025–4035.
[14] H. Lee, S. H. Hong, *Appl. Catal. A* **2018**, *560*, 21–27.
[15] H. Lee, Y. Joe, H. Park, *Catal. Commun.* **2019**, *121*, 15–18.
[16] Y. Zhu, V. H. Rawal, *J. Am. Chem. Soc.* **2012**, *134*, 111–114.
[17] J. J. Race, A. L. Burnage, T. M. Boyd, A. Heyam, A. J. Martínez-Martínez, S. A. Macgregor, A. S. Weller, *Chem. Sci.* **2021**, *12*, 8832–8843.
[18] M. Kranenburg, Y. E. M. Van Der Burgt, P. C. J. Kamer, P. W. N. M. Van Leeuwen, K. Goubitz, J. Fraanje, *Organometallics* **1995**, *14*, 3081–3089.
[19] G. M. Adams, A. S. Weller, *Coord. Chem. Rev.* **2018**, *355*, 150–172.
[20] J. Yin, M. P. Rainka, X.-X. Zhang, S. L. Buchwald, *J. Am. Chem. Soc.* **2002**, *124*, 1162–1163.
[21] G. Zhang, J. Wang, C. Guan, Y. Zhao, C. Ding, *Eur. J. Org.* **2021**, *2021*, 810–813.
[22] T. Ohshima, Y. Miyamoto, J. Ipposhi, Y. Nakahara, M. Utsunomiya, K. Mashima, *J. Am. Chem. Soc.* **2009**, *131*, 14317–14328.
[23] J. Barwick-Silk, S. Hardy, M. C. Willis, A. S. Weller, *J. Am. Chem. Soc.* **2018**, *140*, 7347–7357.
[24] G. L. Moxham, H. E. Randell-Sly, S. K. Brayshaw, R. L. Woodward, A. S. Weller, M. C. Willis, *Angew. Chem. Int. Ed.* **2006**, *45*, 7618–7622; *Angew. Chem.* **2006**, *118*, 7780–7784.
[25] G. L. Moxham, H. Randell-Sly, S. K. Brayshaw, A. S. Weller, M. C. Willis, *Chem. Eur. J.* **2008**, *14*, 8383–97.
[26] D. E. Ryan, K. A. Andrea, J. J. Race, T. M. Boyd, G. C. Lloyd-Jones, A. S. Weller, *ACS Catal.* **2020**, *10*, 7443–7448.
[27] G. M. Adams, D. E. Ryan, N. A. Beattie, A. I. Mckay, G. C. Lloyd-Jones, A. S. Weller, *ACS Catal.* **2019**, *9*, 3657–3666.
[28] J. F. Hooper, A. B. Chaplin, C. González-Rodríguez, A. L. Thompson, A. S. Weller, M. C. Willis, *J. Am. Chem. Soc.* **2012**, *134*, 2906–2909.
[29] B. C. Hamann, J. F. Hartwig, *J. Am. Chem. Soc.* **1998**, *120*, 3694–3703.
[30] J. Wang, G. Meng, K. Xie, L. Li, H. Sun, Z. Huang, *ACS Catal.* **2017**, *7*, 7421–7430.
[31] S. Raoufmoghaddam, E. Drent, E. Bouwman, *ChemSusChem* **2013**, 6, 1759–1773.
[32] Y. Jiao, M. S. Torne, J. Gracia, J. W. Niemantsverdriet, P. W. N. M. Van Leeuwen, *Catal. Sci. Technol.* **2017**, *7*, 1404–1414.
[33] J. Holz, K. Rumpel, A. Spannenberg, R. Paciello, H. Jiao, A. Börner, *ACS Catal.* **2017**, *7*, 6162–6169.
[34] C. J. A. Osborn, F. H. Jardine, J. F. Young, G. Wilkinson, J. R. Shapley, R. R. Schrock, J. A. Osborn, *J. Am. Chem. Soc.* **1969**, *91*, 2816–2817.
[35] R. R. Schrock, J. A. Osborn, *J. Am. Chem. Soc.* **1976**, *98*, 4450–4455.
[36] J. E. Barquera-Lozada, A. Obenhuber, C. Hauf, W. Scherer, *J. Phys. Chem. A* **2013**, *117*, 4304–4315.
[37] M. Lankelma, V. Vreeken, M. A. Siegler, J. I. Van Der Vlugt, *Inorganics* **2019**, *7*, 28.
[38] W.-N. Chou, M. Pomerantz, *J. Org. Chem.* **1991**, *56*, 2762–2769.
[39] S. A. Hauser, I. Prokes, A. B. Chaplin, *Chem. Commun.* **2015**, *51*, 4425–4428.
[40] H. Schmidbaur, A. Schier, *Chem. Soc. Rev.* **2012**, *41*, 370–412.
[41] H. Plenio, *Chem. Rev.* **1997**, *97*, 3363–3384.
[42] T. Tuttle, J. Gräfenstein, D. Cremer, *Chem. Phys. Lett.* **2004**, *394*, 5–13.
[43] J.-C. Hierso, *Chem. Rev.* **2014**, *114*, 4838–4867.
[44] F. B. Mallory, C. W. Mallory, K. E. Butler, M. B. Lewis, A. Q. Xia, E. D. Luzik, L. E. Fredenburgh, M. M. Ramanjulu, Q. N. Van, M. M. Francl, D. A. Freed, C. C. Wray, C. Hann, M. Nerz-Stormes, P. J. Carroll, L. E. Chirlian, *J. Am. Chem. Soc.* **2000**, *122*, 4108–4116.
[45] A through-bond coupling, ^6J(FF), would be expected to be significantly smaller. See ref. 44.
[46] A. G. Orpen, *Chem. Soc. Rev.* **1993**, *22*, 191–197.

[47] W. Goertz, W. Keim, D. Vogt, U. Englert, M. D. K. Boele, L. A. Van Der Veen, P. C. J. Kamer, P. W. N. M. Van Leeuwen, *J. Chem. Soc. Dalton Trans.* **1998**, 2981–2988.
[48] D. Pingen, T. Lebl, M. Lutz, G. S. Nichol, P. C. J. Kamer, D. Vogt, *Organometallics* **2014**, *33*, 2798–2805.
[49] K. Stanek, B. Czarniecki, R. Aardoom, H. Rüegger, A. Togni, *Organometallics* **2010**, *29*, 2540–2546.
[50] M. Brookhart, M. L. H. Green, G. Parkin, *PNAS* **2007**, 104, 6908.
[51] A. Meißner, E. Alberico, H.-J. Drexler, W. Baumann, D. Heller, *Catal. Sci. Technol.* **2014**, *4*, 3409–3425.
[52] R. J. Pawley, G. L. Moxham, R. Dallanegra, A. B. Chaplin, S. K. Brayshaw, A. S. Weller, M. C. Willis, *Organometallics* **2010**, *29*, 1717–1728.
[53] P. Ren, S. D. Pike, I. Pernik, A. S. Weller, M. C. Willis, *Organometallics* **2015**, *34*, 711–723.
[54] A. I. Mckay, J. Barwick-Silk, M. Savage, M. C. Willis, A. S. Weller, *Chem. Eur. J.* **2020**, *26*, 2883–2889.
[55] S. D. Pike, M. R. Crimmin, A. B. Chaplin, *Chem. Commun.* **2017**, *53*, 3615–3633.
[56] P. S. Pregosin, *NMR in Organometallic Chemistry* Wiley, Zurich, **2012**.
[57] Spin simulation of the $^{31}P\{^{1}H\}$ spectrum only recreated the second order form if the chemically equivalent ^{31}P nuclei, *trans* to the hydride, couple to one another with *J*(PP) of 42 Hz.
[58] A. T. Lubben, J. S. Mcindoe, A. S. Weller, *Organometallics* **2008**, *27*, 3303–3306.
[59] J. H. Bowie, *Environ. Health Perspect.* **1980**, *36*, 89–95.
[60] J. H. B. Dennis, J. Underwood, *J. Chem. Soc. Perkin Trans. 2* **1977**, 1670–1674.
[61] An alternative interpretation is that there is a filled M···M antibonding orbital and thus no formal M–M bond. See: J. C. Green, M. L. H. Green, G. Parkin, *Chem. Commun.* **2012**, 48, 11481–11503.
[62] A. J. Pontiggia, A. B. Chaplin, A. S. Weller, *J. Organomet. Chem.* **2011**, *696*, 2870–2876.
[63] M. C. Haibach, D. Y. Wang, T. J. Emge, K. Krogh-Jespersen, A. S. Goldman, *Chem. Sci.* **2013**, *4*, 3683–3692.
[64] P. Ren, S. D. Pike, I. Pernik, A. S. Weller, M. C. Willis, *Organometallics* **2015**, *34*, 711–723.
[65] S. K. Furfari, B. E. Tegner, A. L. Burnage, L. R. Doyle, A. J. Bukvic, S. A. Macgregor, A. S. Weller, *Chem. Eur. J.* **2021**, *27*, 3177–3183.
[66] K. T. Chan, G. S. M. Tong, W.-P. To, C. Yang, L. Du, D. L. Phillips, C.-M. Che, *Chem. Sci.* **2017**, *8*, 2352–2364.
[67] B. Guzel, M. A. Omary, J. P. Fackler, A. Akgerman, *Inorg. Chim. Acta* **2001**, *325*, 45–50.

Manuscript received: March 21, 2022
Revised manuscript received: April 23, 2022
Accepted manuscript online: May 6, 2022

RESEARCH ARTICLE

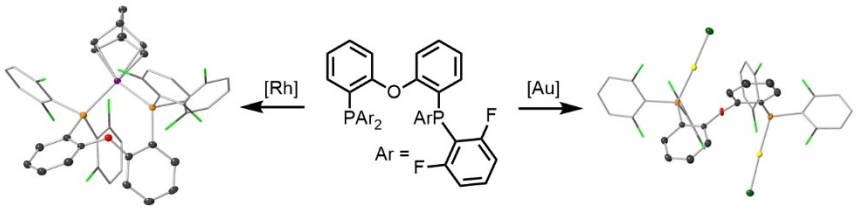

J. J. Race, M. J. Webb, T. Morgan Boyd, Prof. A. S. Weller**

A *ortho*-fluorine substituted DPEphos ligand has been synthesized: *o*-F,F-DPEphos. The influence of the *ortho*-substitution is highlighted by the comparison of the aurophilic interactions in Au_2Cl_2(o-R,R-DPEphos) and the hydrogenation product from [Rh(*o*-R,R-DPEhphos)(NBD)][BAr^F_4] complexes (R═H or F). An unexpected dicationic dimer of *o*-H,H-DPEphos with an agostic C–H group is revealed for the latter.